

# RF DIPOLE CRAB CAVITY TESTING FOR HL-LHC

N. Valverde Alonso\*, R. Calaga, S.J. Calvo, O. Capatina, A. Castilla<sup>1</sup>, M. Chiodini, C. Duval<sup>†</sup>, L.M.A. Ferreira, M. Gourragne, P.J. Kohler, T. Mikkola, J.A. Mitchell, E. Montesinos, C. Pasquino, G. Pechaud, N. Stapley, M. Therasse, K. Turaj, J.D. Walker  
CERN, Geneva, Switzerland

<sup>1</sup>also at Lancaster University, Lancaster, United Kingdom

## Abstract

RF Crab Cavities are an essential element of the High Luminosity LHC (HL-LHC) upgrade at CERN. Two RF dipole crab cavities used for the compensation of the horizontal crossing angle were recently manufactured and integrated into a titanium helium tank and equipped with RF ancillaries necessary for the beam operation. The two cavities will be integrated into a cryomodule in collaboration with UK-STFC and tested with proton beams in the SPS in 2023. This paper will highlight the RF measurements during the final manufacturing steps, surface preparation and cavity performance at 2 K.

## INTRODUCTION

RF Crab Cavities are required for the HL-LHC upgrade [1] at CERN to transversely rotate the bunches and re-establish the head-on collisions at the interaction point (IP). This rotation compensates for the geometric factor and increases the peak luminosity by more than 65%. In the HL-LHC, the two IPs have alternating crossing angle, one horizontal (ATLAS) and one vertical (CMS). For the horizontal crossing, the RF dipole superconducting crab cavity will provide the crabbing manipulation to compensate for the horizontal crossing angle. A two cavity cryomodule is under construction towards a test with proton beams, hosting two RF dipole (RFD) crab cavities (see Fig. 1) [2]. The beam tests are planned for 2023 in the CERN-SPS machine. While the cryomodule integration will be done at the UK-STFC premises, the two bulk niobium, jacketed and dressed RFD cavities were fabricated and tested at CERN.

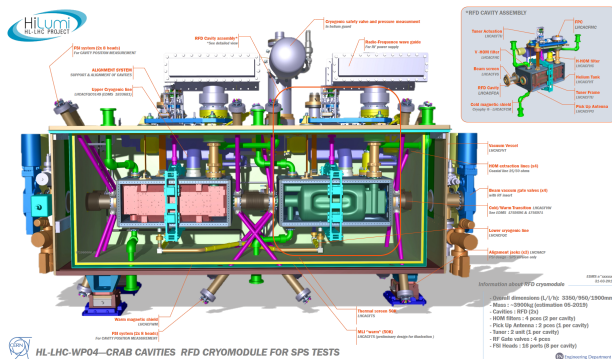


Figure 1: Cross section of the RFD cryomodule hosting two cavities (courtesy CERN EN-MME).

\* Nuria.Valverde.Alonso@cern.ch

<sup>†</sup> from consortium AL-40/30

Due to their exotic geometry, compact deflectors, such as the RFD cavities (see Fig. 2), follow a complex manufacturing procedure [3]. To ensure that the cavities are at the correct range of frequency during operation, careful calculations are performed to determine a “recipe” that lays out the frequency requirements for the different manufacturing and processing steps. To enforce this, rigorous RF controls are carried out during the identified key steps of the cavity life. The surface treatment and preparations for the cold test,

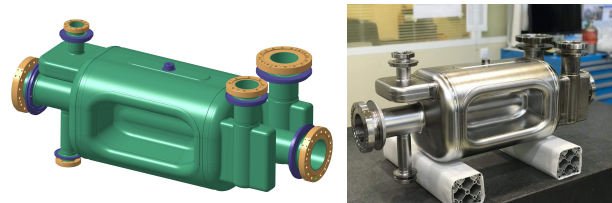


Figure 2: Left: The RFD cavity geometry. Right: RFD cavity manufactured from high RRR Niobium.

as well as results and performance will be presented in the following sections. This paper will also address some of the main challenges for preparing and processing RFD cavities in the final section and will close with some discussion and remarks.

## FREQUENCY TUNING OF SUB-COMPONENTS

Table 1 lists the target frequency requirements for the crabbing mode at different steps of the production process of RFD cavities for the HL-LHC, including buffered chemical polishing (BCP), heat treatment (HT), vertical cold tests (VCT) for the bare cavity, as well as for the dressed cavity (DC), which is defined as the jacketed cavity with all the couplers and antennas installed. Further details on the manufacturing of the couplers can be found in Ref. [4].

All the values in Table 1 are expected to be measured within a  $\pm 0.05$  MHz error threshold.

The first RF controls are visual inspections carried out throughout the deep drawing and welding of the individual sub assemblies, such as: ports, pipes, capacitive plates, etc. The first RF measurement at ambient temperature is possible upon the completion of the three main sub-assemblies (i.e.) the two end caps and the mid body (see Fig. 3).

The end caps were trimmed to their nominal length, and their edges machined to nominal thickness with calibration of the edge face to reach the specified planarity. During each fabrication step, metrology controls are performed to ensure

Table 1: Frequency Recipe for the RFD’s Fundamental Mode

Step	Frequency	Units
After trim (pre-welding)	400.11	MHz
After welding	400.26	MHz
After bulk BCP + HT (~120 μm)	400.20	MHz
After light BCP (~30 μm)	400.19	MHz
At VCT (vacuum, 4.5 K)	400.70	MHz
At VCT (vacuum, 2 K)	400.85	MHz
After jacketing (in air, 300 K)	400.19	MHz
After dressing (vac., 300 K)	400.13	MHz
DC w/tuner ON (vac., 2 K)	400.86	MHz
At operation (vac., 2 K)	400.79	MHz

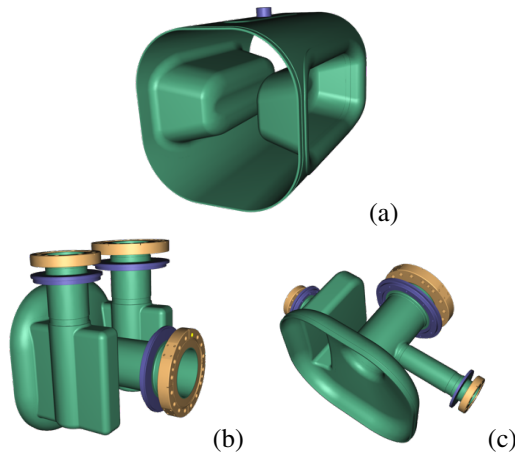


Figure 3: RFD main sub assemblies: (a) mid body, (b) and (c) end caps.

that the dimensions and shapes are within tolerance. The mid-body is kept with a symmetrical extra length of 20 mm on both sides, with respect to the design length.

The trim tuning strategy entails stacking the three sub assemblies vertically and hold them in place by compression using metallic plates guided by threaded rods.

A minimum of three full symmetrical tightening and loosening cycles are performed to ensure the optimal RF contact of the three sub assemblies. The maximum compression is limited to a minimum elastic deformation. The optimal compression force is determined by the measured loaded Q-factor of the stack, while ensuring a minimum shift in frequency.

The mid-body is symmetrically trimmed with frequency measurements repeated until the desired frequency target is reached. If the frequency target is not reached close to the design length, a re-tuning of the cavity by means of pulling or pushing the capacitive elements in the mid body is carried out. This step is typically required if the frequency deviation is large due to an important deviation from its nominal shape. Figure 4 shows the trim tuning campaign of the two RF dipoles (labeled RFD1 and RFD2, respectively). A third RFD cavity to be used as a spare (labeled RFD3),

is presently undergoing frequency tuning and is included in Fig. 4 at its current status.

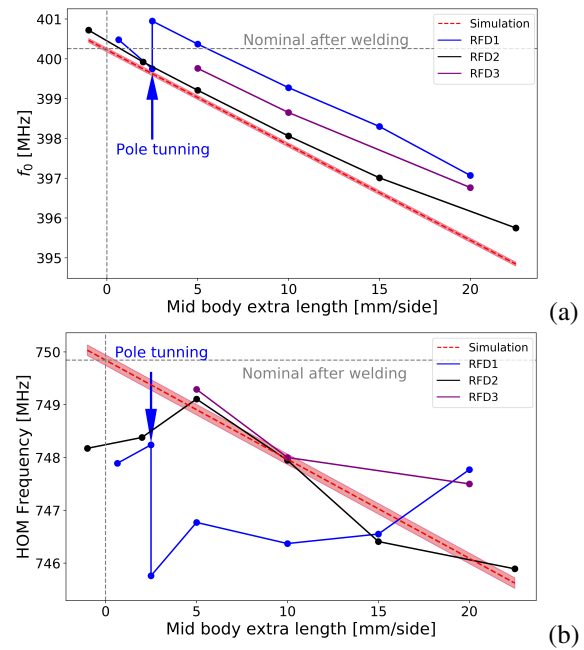


Figure 4: Trim tuning comparison for three different RFD cavities for (a) the fundamental and (b) the high power HOM.

Figure 4(a) shows the simulated values of the fundamental frequency, for the different mid body extra lengths (red-dashed line), and the measurements of three different RFD cavities manufactured at CERN. Figure 4(b) shows the same frequency evolution during the trim tuning for the most important higher order mode (HOM) at ~750 MHz. During the trim tuning of the first cavity (RFD1) the frequency was corrected by pushing the capacitive elements, or poles, by about 560 μm inwards. The difference between the measured frequency with respect to the expected one for this cavity, was consistent with an observed separation of the poles (~580 μm), with respect to the ideal shape. By correcting the pole distance to the design value, both the frequency ( $\Delta f_0 \sim -1.2$  MHz) and the shape were brought back to within the tolerance.

After the frequency tuning steps, the first end cap consisting of the fundamental power coupler (FPC) and horizontal HOM (HHOM) ports are welded to the main body (see Fig. 3(b)). This is followed by a final stack with the remaining end cap and a frequency measurement to determine the shift due to the weld (i.e. material shrinkage, under-bead, shape deformation, etc.). The last end cap consisting of the pickup and vertical HOM (VHOM) ports (see Fig. 3(c)) is welded and the frequency is recorded for the final assembly.

Figure 5 shows the measured frequencies at some of the steps following the frequency tuning campaign for (a) the cavities’ fundamental and (b) the high power HOM. The red dashed line represent the calculated values and the red shaded zone represent the assigned tolerances of ±50 kHz

for the fundamental and  $\pm 100$  kHz for the “750 MHz” HOM.

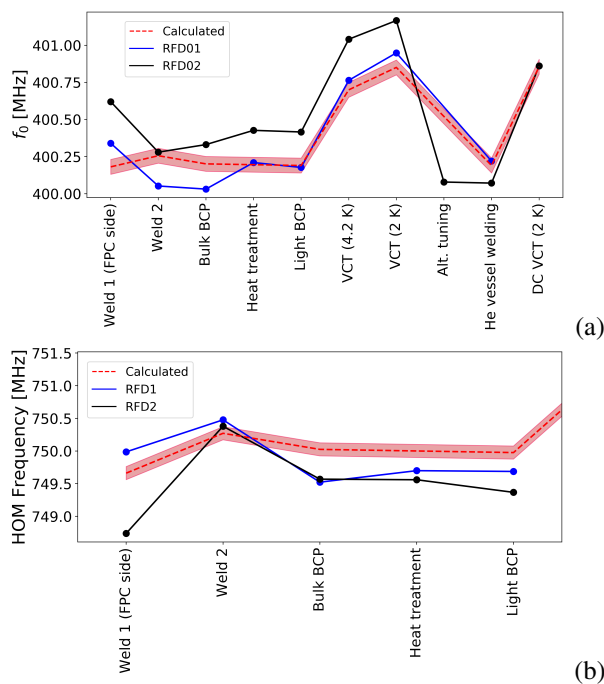


Figure 5: Frequency evolution of two RFD cavities manufactured and prepared at CERN. For (a) the fundamental and (b) the high power HOM.

The frequencies of the fundamental, as well as relevant HOMs are recorded throughout the cavity life for the different VCTs, alternative pole tunings (if deemed necessary), transport, etc., up to installation in the machine. This ensures that the cavities will reach both performance requirements, as well as frequency specifications during operation in the machine, without sacrificing on the tuning range to correct for manufacturing and processing errors.

## SURFACE PREPARATION

A rotational buffer chemical polishing (BCP) facility was built at CERN for surface etching of the HL-LHC crab cavities to ensure a uniform removal of material along their complex shape. Details of this new facility are available in Ref. [5]. The aforementioned RFD1 and RFD2 bare cavities were etched at a temperature between 13 °C and 17 °C, with a flow rate of 4 to 14 lpm. The cavities were processed in a horizontal position, while rotating axially at 1 rpm. The direction of the flow is from one beam port to the other.

Two to three BCP steps were done on each cavity with a final light BCP. During each BCP step, ultrasound thickness measurements at 39 points around the cavity and RF measurements are performed to control the thickness removal. The total average thickness removal was 261  $\mu\text{m}$  for RFD1 and 226  $\mu\text{m}$  for RFD2, before the cold tests. The frequency shifts are presented in Fig. 5. After the bulk removal and before the light BCP, the cavity was submitted to a heat treatment of 650 °C for 24 h to remove hydrogen precipitation

on the cavity surface. Figure 6 shows, as an example, the accumulated removal for each chemical etching step performed on the RFD1 cavity, as a function of the position of the thickness measurement on the cavity.

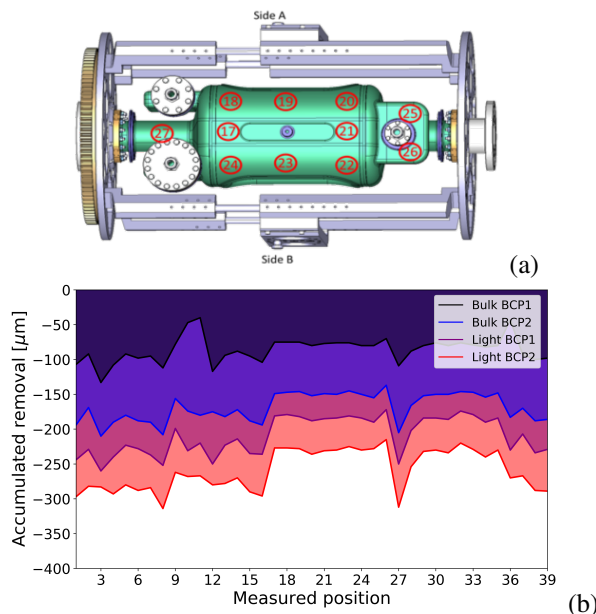


Figure 6: (a) Example of locations measured in the cavity and (b) the accumulated removal on RFD1 for the different chemical polishing steps.

## RF TEST PREPARATION AT 2 K

### Clean Room Assembly

After the surface etching and high temperature heat treatment, the cavities are degreased, followed by a low pressure rinse using de-ionized (DI) water ( $<15 \text{ M}\Omega\cdot\text{cm}$ ). The cavity is subject to a final light rinse with ethanol to accelerate the drying process.

Prior to clean room assembly, a high pressure water rinsing (HPR) of the cavity is performed with ultra pure DI water (21 °C, 18.2  $\text{M}\Omega\cdot\text{cm}$ , pH 6, and total organic carbon content (TOC)  $<20$  ppb) at  $\sim 100$  bar. The cavity is installed vertically in the HPR cabinet on a rotatable table while the HPR wand performs controlled vertical strokes until the outlet water reaches the desired particle count levels. The HPR is typically considered done once the outlet water measured levels reach  $\leq 10,000$  counts/ml for 0.1  $\mu\text{m}$  particles,  $\leq 1,000$  counts/ml for 0.2  $\mu\text{m}$  particles,  $\leq 100$  counts/ml for 0.5  $\mu\text{m}$  particles,  $\leq 10$  counts/ml for 1  $\mu\text{m}$ , TOC  $<50$  ppb, and resistivity  $\sim 0.95 \text{ M}\Omega\cdot\text{cm}$ .

Figure 7 presents a global summary of one of the cavity rinsing campaigns. It is important to note that the particle counts become saturated at around 20,000 counts/ml. Therefore, levels beyond this limit will not be measured and appear as a flat top. Additional spikes on the observed counts correspond to the water jet location at the cavity's top and bottom beam ports. This results in spraying water

Content from this work may be used under the terms of the CC BY 4.0 licence (© 2022). Any distribution of this work must maintain attribution to the author(s), title of the work, publisher, and DOI

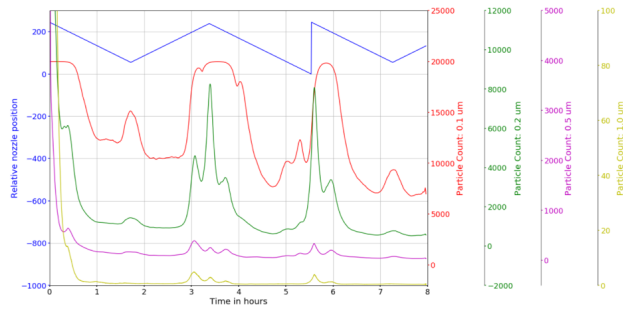


Figure 7: Particle count summary of the outlet water during an HPR of RFD1 cavity; the curves on the graph show averaged values.

on to the cabinet walls which does not reflect the quality of the cavity's inner surface. For the HL-LHC RFD cavity geometry, a  $\sim 7$  h HPR duration was established empirically as a sufficient rinsing duration.

The HPR cabinet's second door has direct access to the ISO 4 cleanroom, where the cavity is placed for drying under laminar flow. The cavity is assembled with the required hook-type antennas and closed with Nb-coated stainless steel (316LN) flanges and OFE copper gaskets. A special lifter was used to manipulate the cavity due to its weight.

### Cold Test Set Up

The RF tests at 2 K are carried out in a vertical cryostat (V4) at the SM18 facilities. During the cavity tests, the outer surface of the cavity is equipped with contact CERNOX<sup>®</sup> temperature sensors, three single-axis magnetic flux probes, and radiation monitors to measure the X-rays. The cryostat is also equipped with magnetic compensation coils to keep the ambient field to  $0.5 \mu\text{T}$ . For the cold test of the bare cavities, a stiffening frame made of titanium was installed around the cavity to simulate the stiffness of the helium tank. This prevents unwanted deformations during cool down and closely mimics the final jacketed cavity. Throughout the assembly process in the vertical cryostat, the frequency of the cavity was constantly monitored. Once the cavity is connected to the cryostat pumping line, a low temperature baking is performed at  $120^\circ\text{C}$  for 48 h.

### Cool Down Process

The cooldown process was divided into three stages to limit the differential contractions of the cavity and avoid plastic deformation. In the first stage, from 300 to 130 K, the cavity and cryostat are cooled by cooling the thermal shields of the cryostat. The maximum gradient across the cavity is  $\approx 10$  K and the process takes  $\approx 36$  h. In the second stage, the cryostat is filled with liquid helium to reach 4.5 K in approximately 3 h. In the third stage, the cryostat is pumped down to 2 K.

## RF TEST RESULTS

A performance specification was outlined for the dressed crab cavities for their use in the HL-LHC [6]. To reach the

target specification, a minimum of three RF tests at 2 K, are necessary to validate their performance at different stages: bare, jacketed, and dressed cavity. At each test, the cavities systematically presented multipacting at low transverse voltages below 2 MV (i.e. 1 MV and 1.9 MV). These barriers required some RF conditioning, using pulse and amplitude modulation, to allow stable conditions for RF measurements.

### Bare Cavity Results

The RF performance test results for RFD1 and RFD2 bare cavities are shown in Fig. 8.

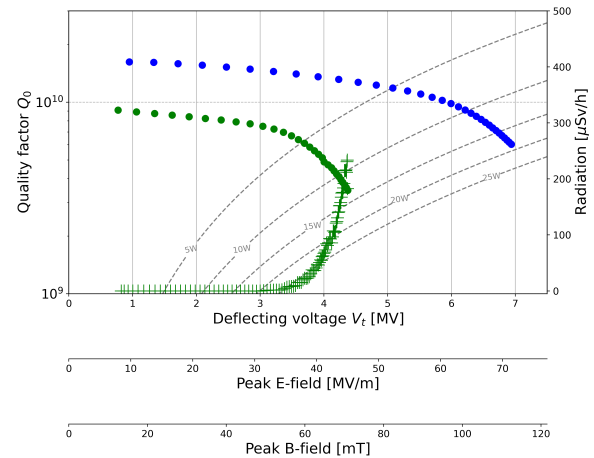


Figure 8: Performance results of the bare RFD cavities (in green-RFD1 and in blue-RFD2).

At the quench limit, the RFD1 cavity reached a maximum transverse voltage equal to 4.4 MV ( $Q_0 = 3.5 \times 10^9$ ) and peak fields of  $E_{peak} = 44.9$  MV/m and  $B_{peak} = 70.7$  mT. The field emission onset was observed at 3 MV and remained at a low level, less than  $0.5 \mu\text{Sv/h}$ . At low field, the cavity's  $Q_0$  was  $9 \times 10^9$ , which corresponds to a surface resistance of  $11.5 \text{ n}\Omega$ . The RFD2 cavity exceeded the nominal deflecting voltage (3.4 MV) with a factor two margin (up to 6.9 MV,  $Q_0 = 6 \times 10^9$ ) and peak fields of  $E_{peak} = 71$  MV/m and  $B_{peak} = 112$  mT. No field emission measurement was available during the RFD2 test due to a malfunction of the radiation sensor. However, the low  $Q$  slope indicates the onset to be well beyond 5 MV. The residual surface resistance of the RFD2 cavity was estimated to be  $6 \text{ n}\Omega$  from the calculated geometry factor and the measured intrinsic  $Q_0$  as a function of temperature for a fixed low field value (see Fig. 9).

The measured Lorentz force detuning coefficient (LFD) for the RFD1 was  $-735 \text{ Hz/MV}^2$ , and  $-720 \text{ Hz/MV}^2$  for the RFD2, as can be appreciated in Fig. 10.

The pressure sensitivity of the RFD2 bare cavity was estimated to be  $-105 \text{ Hz/mbar}$ , using measurements of the cavity's frequency during the warm-up at low field.

### Jacketed Cavity Results

The jacketed cavity consists of a titanium helium vessel in bolted design configuration with welds for leak tightness.

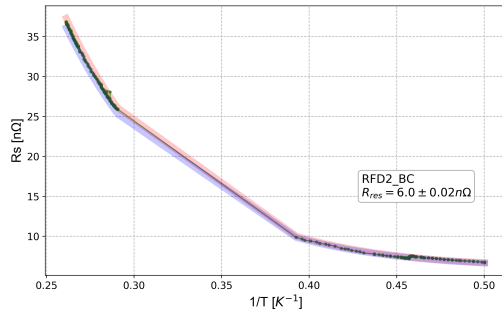


Figure 9: Measured surface resistance of the bare RFD2 cavity, as a function of temperature.

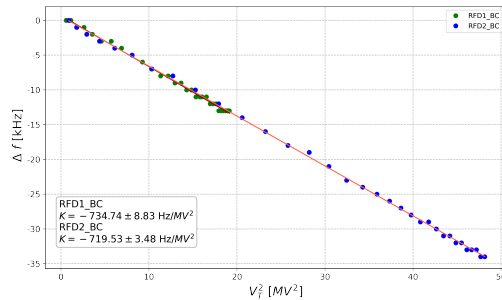


Figure 10: Measured Lorentz Force coefficients for both bare RFD cavities (in green-RFD1 and in blue-RFD2).

An internal magnetic shield is used between the cavity and the helium vessel to provide a strong suppression of the ambient magnetic field.

The jacketed cavities were subjected to an HPR, clean-room assembly of antennas and Nb-coated flanges, followed by a low temperature bake out procedure, similar to the bare cavity. Due to the presence of a passive magnetic shield inside the helium vessel, active magnetic field compensation was not used during the cold test. All inlets and outlets of the helium vessel were kept open to allow sufficient cooling of the cavity body.

For the RFD1, a second light BCP of  $\sim 50 \mu\text{m}$  was performed just before the helium vessel assembly (see Fig.5) in view of performance increase closer to the RFD2. The test of the jacketed cavity performed well beyond the specification i.e.  $V_t = 5 \text{ MV}$ , but dropped to the lower value of 3.6 MV during pulse conditioning. This drop was correlated with the onset of the exponential field emission rise below 3 MV. Therefore, the cavity underwent an additional HPR treatment and was re-tested.

The RFD1 jacketed cavity performance was recovered during the second test to 5 MV (with  $Q_0 = 3.8 \times 10^9$ ) without observing a quench (see Fig. 11). The corresponding maximum peak electric and magnetic surface fields were  $E_{peak} = 51.6 \text{ MV/m}$  and  $B_{peak} = 81.3 \text{ mT}$ , respectively. The cavity was tested stably in CW-mode for at least 3 hours at  $V_t = 4.3 \text{ MV}$ , no increase of radiation, temperature, nor

quenches were observed. At low fields, the cavity's  $Q_0$  was  $1.5 \times 10^{10}$ . The residual surface resistance was 7 nΩ. The measured LFD coefficient and pressure sensitivity were -717 Hz/MV<sup>2</sup> and -99 Hz/mbar respectively.

The RFD2 cavity was mechanically tuned prior to the assembly of the helium tank (see alternative tuning in Fig. 5). The results obtained during the jacketed cavity tests are in good agreement with the bare cavity results. This cavity reached a maximum transverse voltage equal to 7 MV,  $Q_0 = 5 \times 10^9$ , and peak fields of  $E_{peak} = 72 \text{ MV/m}$  and  $B_{peak} = 112 \text{ mT}$ . The field emission onset was observed just below 5 MV (see Fig. 11). The residual surface resistance of the cavity was estimated to be 6.8 nΩ, the measured LFD coefficient -675 Hz/MV<sup>2</sup>, and the pressure sensitivity -104 Hz/mbar (see Fig. 12).

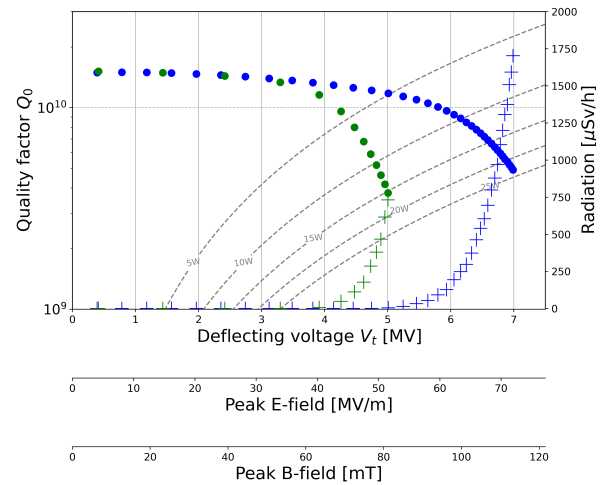


Figure 11: Performance results for both jacketed RFD cavities (in green-RFD1 and in blue-RFD2).

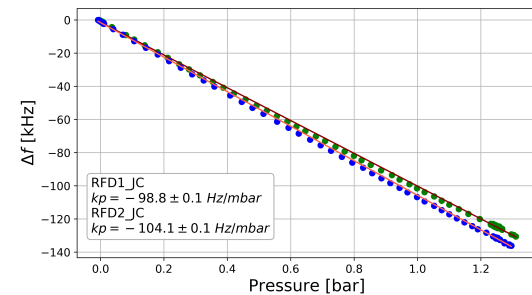


Figure 12: Pressure sensitivity of both jacketed RFD cavities (in green-RFD1 and in blue-RFD2).

### Dressed Cavity Results

The RFD2 jacketed cavity was HPRed and equipped with HOM couplers and the field antenna in its final configuration before cryostating. Due to risk represented by the RF feedthroughs and other coupler elements, a low temperature (120 °C) bake-out was omitted. For this test, the horizontal

Content from this work may be used under the terms of the CC BY 4.0 licence (© 2022). Any distribution of this work must maintain attribution to the author(s), title of the work, publisher, and DOI

HHOM coupler, with an external coupling to the fundamental  $Q_{ext1} \approx 1 \times 10^{10}$ , was used as input probe to couple the RF power. A special pickup probe was inserted into the beam port on the FPC side, and provided external coupling  $Q_{ext2} \approx 9 \times 10^{11}$ . The dressed cavity was tested fully immersed in liquid helium, as it was done for the jacketed cavities. The RFD2 cavity surpassed the nominal deflecting voltage of 3.4 MV, reaching slightly beyond 5 MV. Due to safety reasons, higher gradients up to the quench field were not pursued. No significant field emission was observed, up to almost 4 MV. The RF test results of RFD2-DC are shown in Fig. 13.

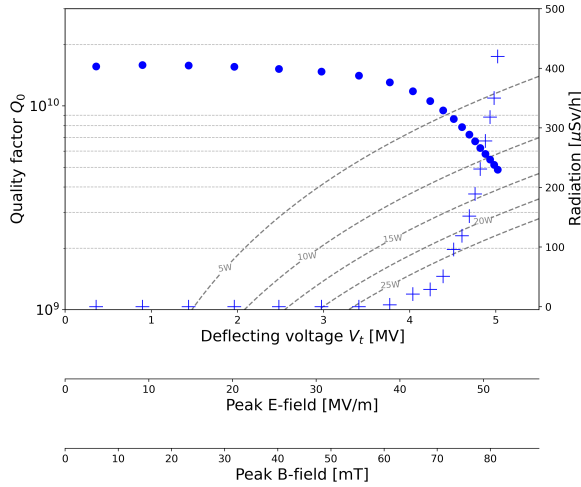


Figure 13: Performance results of the dressed RFD2 cavity.

The residual surface resistance of the cavity was estimated to be  $6.5 \text{ n}\Omega$  from the calculated geometry factor and the measured intrinsic Q at low fields which is consistent with previous tests without HOM couplers. The LFD coefficient was  $-713 \text{ Hz/MV}^2$  and the pressure sensitivity, measured during the warm-up at a fixed low field, was  $-110 \text{ Hz/mbar}$ , in agreement with previous results.

The RFD1 dressed cavity is undergoing preparations for its subsequent cold test. Table 2 presents the performance summary for the different VCT performed to date, including the specification parameters for their comparison. Both the jacketed RFD1 and the dressed RFD2 cavity measurements were purposely stopped at 5 MV, following the established executive safety protocol.

## CHALLENGES AND DISCUSSION

The modern manufacturing of high performing bulk niobium RF cavities comes with many standard challenges, starting from material procurement, all the way to cavity surface processing. In particular, complex geometries, like the compact transverse deflectors employed as crab cavities for the HL-LHC, require good quality assurance practices. For this reason, CERN has established a tight series of quality controls for the entire cavity production span. The described frequency recipe is an example of this. The procedures

themselves were continuously assessed and improved when deemed necessary. After the production of two double quarter wave (DQW) and the two RF dipoles (RFD), including the world record performance results and reproducibility, CERN has launched the knowledge transfer to industry, jointly with its collaborators in the U.S., to fabricate the series HL-LHC crab cavities. The efforts carried out by the US-AUP on HL-LHC RFD prototypes is presented in Ref. [7].

Several important lessons were learned during the assembly, preparation, and testing of the RFD cavities. The high field Q-slope and the maximum field reach is almost always dominated by the presence of field emission in cavities tested at CERN. HPR was proven to be an effective method to recover a degraded cavity performance due to early onset of field emission. The jacketed RFD1 cavity performance was successfully restored after using the HPR treatment, as seen in Fig. 14.

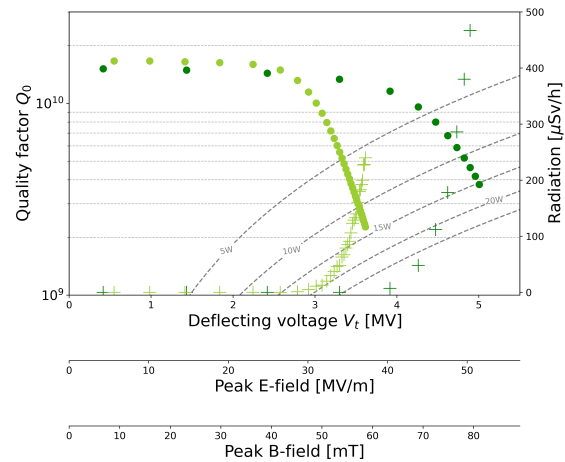


Figure 14: The impact of HPR on the improvement of the jacketed RFD1 cavity performance, in light green-before and in dark green-after the HPR treatment.

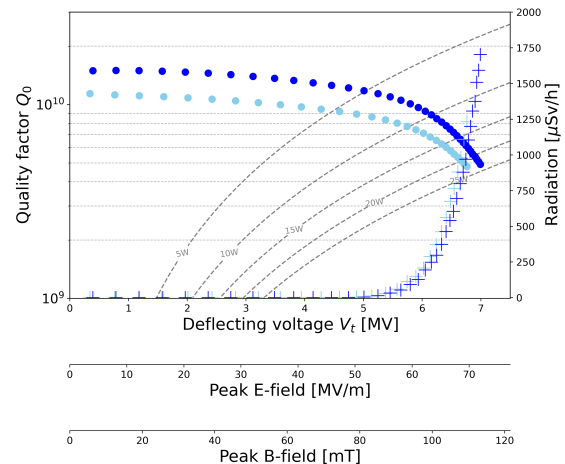


Figure 15: Performance results of the jacketed RFD2 cavity before (light blue) and after (blue) the thermal cycle.

Table 2: Summary of Cavity Test Performance

Parameters	Specification	RFD1 BC	RFD2 BC	RFD1 JC	RFD2 JC	RFD2 DC
Resonant freq. [MHz]	400.79±0.15*	400.95	401.17	400.96	400.86	400.86
Max $V_t$ [MV]	≥4.1	4.36	6.9	5	7	5
$Q_0$ at 4.1 MV	≥3.9×10 <sup>9</sup>	4.6×10 <sup>9</sup>	1.3×10 <sup>10</sup>	1.1×10 <sup>10</sup>	1.3×10 <sup>10</sup>	1.2×10 <sup>10</sup>
LFD coeff.  [Hz/MV <sup>2</sup> ]	≤865	735	720	717	675	713
dF/dp  [Hz/mbar]	≤300	-	105	99	105	110
$P_{diss}$ at 4.1 MV [W]	≤10	8.6	2.1	3.1	3	3.2

\*The manufacturing target was set to 400.85±0.05 MHz, to keep the tuner engaged as default operation set point

During the course of the testing, it was established that a thermal cycle, up to ≈20 K (see Fig. 15), consistently improved the  $Q_0$  of both the jacketed and dressed cavities by ≈25%.

### ACKNOWLEDGMENTS

This research is supported by the HL-LHC project, US DOE through US-AUP and UK-STFC through HL-LHC-UK. The authors thank the members of HL-LHC WP4 (crab cavity) collaboration and CERN departments for their invaluable contributions. Special thanks to the technical support from the superconducting RF and the cryogenics sections for making these tests possible.

### REFERENCES

- [1] O. Bruning and L. Rossi, *The High Luminosity Large Hadron Collider (Advanced series on directions in high energy physics, Volume 24)*. World Scientific, Oct. 2015.
- [2] S. U. De Silva, J. R. Delayen, H. Park, Z. Li, and T. H. Nicol, “Design and prototyping of a 400 MHz RF-dipole crabbing cavity for the LHC high-luminosity upgrade”, in *Proc. 6th Int. Particle Accelerator Conf. (IPAC’15)*, Richmond, VA, USA, May 2015, pp. 3568–3571. doi:10.18429/JACoW-IPAC2015-WEPWI036
- [3] M. Garlasche, “Advanced manufacturing techniques for the fabrication of HL-LHC crab cavities at CERN”, in *Proc. 18th Int. Conf. RF Superconductivity (SRF’17)*, Lanzhou, China, Jul. 2017, pp. 409–414. doi:10.18429/JACoW-SRF2017-TUPB013
- [4] S. Barriere, et al., “HOM couplers and RF antennas for HL-LHC crab cavities: developments for manufacturing”, presented at SRF’21, Grand Rapids, MI, USA, Jun. 2021, paper MOPCAV016, this conference.
- [5] N. Chritin, V. Gebert, R. Ferreira and L. M. Ferreira, “Surface polishing facility for superconducting RF cavities at CERN”, presented at SRF’21, Grand Rapids, MI, USA, Jun. 2021, paper TUPFAV004, this conference.
- [6] L. Alberty *et al.*, “Dressed bulk niobium radio-frequency crab cavities”, *CERN Engineering Specification*, EDMS No.1389669.
- [7] L. Ristori *et al.*, “Development and performance of RFD crab cavity prototypes for HL-LHC AUP”, presented at SRF’21, Grand Rapids, MI, USA, Jun. 2021, paper THPCAV013, this conference.